TOPICAL REVIEW

Twenty-five years of multifractals in fully developed turbulence: a tribute to Giovanni Paladin

To cite this article: G Boffetta *et al* 2008 *J. Phys. A: Math. Theor.* **41** 363001

View the article online for updates and enhancements.

Related content

- Lagrangian statistics in two-dimensional free turbulent convection
  A Bistagnino and G Boffetta

- Extended self-similarity of intermittent turbulence in edge magnetized plasmas
  V.P. Budaev, N. Ohno, S. Masuzaki et al.

- Active and passive fields face to face
  Antonio Celani, Massimo Cencini, Andrea Mazzino et al.

Recent citations

- Beyond Kolmogorov cascades
  Bérengère Dubrulle

- Cascades and transitions in turbulent flows
  A. Alexakis and L. Biferale

- Mesoscopic Transport Events and the Breakdown of Fick's Law for Turbulent Fluxes
  T. S. Hahm and P. H. Diamond
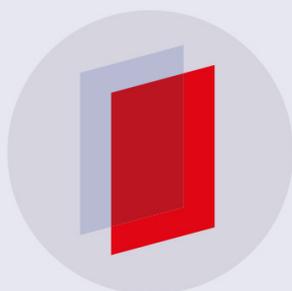
IOP ebooks™

Bringing you innovative digital publishing with leading voices to create your essential collection of books in STEM research.

Start exploring the collection - download the first chapter of every title for free.

TOPICAL REVIEW

Twenty-five years of multifractals in fully developed turbulence: a tribute to Giovanni Paladin

G Boffetta[1], A Mazzino[2] and A Vulpiani[3]

[1] Dipartimento di Fisica Generale, Università di Torino, CNISM and INFN, via P Giuria 1, 10125 Torino, Italy
[2] Dipartimento di Fisica, Università di Genova, CNISM and INFN, via Dodecaneso 33, 16146 Genova, Italy
[3] Dipartimento di Fisica, Università di Roma 'La Sapienza', CNISM and INFN, p.le A Moro 2, 00185 Roma, Italy

E-mail: Angelo.Vulpiani@roma1.infn.it

Abstract

The paper *On the multifractal nature of fully developed turbulence and chaotic systems*, by Benzi *et al* (1984 *J. Phys. A: Math. Gen.* **17** 3521) has been a starting point of many investigations on the different faces of self-similarity and intermittency in turbulent phenomena. Since then, the multifractal model has become a useful tool for the study of small-scale turbulence, in particular for detailed predictions of different Eulerian and Lagrangian statistical properties. On the occasion of the 50th birthday of our unforgettable friend and colleague Giovanni Paladin (1958–1996), we review here the basic concepts and some applications of the multifractal model for turbulence.

PACS numbers: 47.27.Gs, 47.27.eb, 47.53.+n, 05.45.Df, 47.51.+a, 05.10.Gg

(Some figures in this article are in colour only in the electronic version)

1. Introduction

The idea of the multifractal approach to fully developed turbulence has been introduced by Giorgio Parisi and Uriel Frisch during the Summer School *Turbulence and Predictability of Geophysical Fluid Dynamics* held in Varenna in June 1983 [1]. One of us (AV) had the chance to participate in that school and then to coauthor, with R Benzi, G Parisi and G Paladin, the paper published in this journal where the word multifractal appeared for the first time [2].

From a technical point of view the idea of the multifractal is basically contained in the large deviation theory [3, 4], which is an important chapter of the probability theory. However, the introduction of the multifractal description in 1980s had an important role in statistical physics, chaos and disordered systems. In particular, to clarify in a rather neat way that the

usual idea, coming from critical phenomena, that just few scaling exponents are relevant, is wrong, and an infinite set of exponents is necessary for a complete characterization of the scaling features.

As pioneering works which anticipated some aspects of the multifractal approach to turbulence, we can cite the log-normal theory of Kolmogorov [5], the contributions of Novikov and Stewart [6] and Mandelbrot [7].

This paper has no pretense to be a survey of the many applications of the multifractal description in chaos, disordered systems and natural phenomena; for general reviews on these aspects, see [8–10]. For a more mathematically oriented treatment, see [11]. Our aim is a discussion on the use of the multifractal methods in the study of the scaling features of fully developed turbulence.

The paper is organized as follows. Section 2 is devoted to the introduction of the multifractal model of turbulence and its connections with the $f(\alpha)$ versus α formalism introduced by Halsey *et al* [12], and the large deviations theory [3, 4]. In section 3 we discuss the implications of multifractality on Eulerian features, namely the statistical properties of the velocity gradients and the existence of an intermediate dissipative range. Section 4 is devoted to the implications of the multifractal nature of turbulence on Lagrangian statistics. In section 5 we present the Lagrangian acceleration statistics. Section 6 treats the relative dispersion, in particular we discuss the multifractal generalization of the classical Richardson theory. Section 7 is devoted to the multifractal analysis of the dispersion in two-dimensional convection.

2. From Kolmogorov to multifractals

Let us consider the Navier–Stokes equations for an incompressible fluid:

$$\frac{\partial \mathbf{v}}{\partial t} + (\mathbf{v} \cdot \nabla)\mathbf{v} = -\frac{1}{\rho}\nabla p + \nu \Delta \mathbf{v} + \mathbf{F}, \qquad \nabla \cdot \mathbf{v} = 0. \tag{1}$$

Because of the nonlinear structure of the equation, an analytical treatment is a formidable task. For instance, in the 3D case, a theorem for the existence of global solution for arbitrary ν is still missing.

For a perfect fluid (i.e. $\nu = 0$) and in the absence of external forces ($\mathbf{F} = 0$), the evolution of the velocity field is given by the Euler equation, which conserves the kinetic energy. In such a case, introducing an ultraviolet cutoff K_{max} on the wave numbers, it is possible to build up an equilibrium statistical mechanics simply following the standard approach used for the Hamiltonian statistical mechanics. On the other hand, because of the so-called dissipative anomaly [13, 14], in 3D the limit $\nu \to 0$ is singular and cannot be interchanged with $K_{max} \to \infty$, therefore the statistical mechanics of an inviscid fluid has a rather limited relevance for the Navier–Stokes equations at very high Reynolds numbers ($Re = VL/\nu$, where V and L are the typical speed and length of the system, respectively).

In addition, mainly as a consequence of the non-Gaussian statistics, even a systematic statistical approach, e.g. in terms of closure approximations, is very difficult [13, 14].

In the fully developed turbulence (FDT) limit, i.e. $\nu \to 0$, and in the presence of forcing at large scale, one has a non-equilibrium statistical steady state, with an inertial range of scales, where neither energy pumping nor dissipation acts, which shows strong departures from the equipartition [13, 14]. A simple and elegant explanation of the main statistical features of FDT is due to Kolmogorov [15]: in a nutshell, it is assumed the existence of a range of scales where the energy—injected at the scale L—flows down (with a cascade process, as remarked by Richardson [16]) to the dissipative scale $\ell_D \sim L Re^{-3/4}$, where it is dissipated by molecular

viscosity. Since, practically, neither injection nor dissipation takes place in the inertial range, the only relevant quantity is the average energy transfer rate $\bar{\varepsilon}$. Dimensional counting imposes the power-law dependence for the second-order structure function (SF)

$$S_2(\ell) = \langle \delta v_\ell^2 \rangle = \langle (v(x+\ell) - v(x))^2 \rangle \propto \bar{\varepsilon}^{2/3} \ell^{2/3}, \tag{2}$$

where, for the sake of simplicity, we ignore the vectorial nature of the velocity field. The scaling law (2) is equivalent to a power spectrum $E(k) \propto \bar{\varepsilon}^{2/3} k^{-5/3}$ in good agreement with the experimental observations. The original Kolmogorov theory (often indicated as K41) assumes a self-similarity of the turbulent flow. As a consequence, the scaling behavior of higher order structure functions,

$$S_p(\ell) = \langle |v(x+\ell) - v(x)|^p \rangle \sim \ell^{\zeta_p}, \tag{3}$$

is described by a single scaling exponent: $\zeta_p = p/3$.

2.1. The multifractal model

The Navier–Stokes equations are formally invariant under the scaling transformation:

$$\mathbf{x} \to \lambda \mathbf{x}, \qquad \mathbf{v} \to \lambda^h \mathbf{v}, \qquad t \to \lambda^{1-h} t, \qquad \nu \to \lambda^{h+1} \nu,$$

with $\lambda > 0$ (indeed the Reynolds number VL/ν is invariant under the above transformations).

The exponent h cannot be determined with only symmetry considerations, nevertheless there is a rather natural candidate: $h = 1/3$. Such a value of the exponent is suggested by the dimensional argument of the K41 and also, and more rigorously, by the so-called '4/5 law', an exact relation derived by Kolmogorov from the Navier–Stokes equations [13, 17], which, under the assumption of stationarity, homogeneity and isotropy, states

$$\langle \delta v_{||}^3(\ell) \rangle = -\frac{4}{5} \bar{\varepsilon} \ell, \tag{4}$$

where $\delta v_{||}(\ell)$ is the longitudinal velocity difference between two points at a distance ℓ.

We can say that the K41 theory corresponds to a global invariance with $h = 1/3$ and therefore $\zeta_p = p/3$. This result is in disagreement with several experimental investigations [13, 18] which have shown deviations of the scaling exponents from $p/3$. This phenomenon, which goes under the name of intermittency [13], is a consequence of the breakdown of self-similarity and implies that the scaling exponents cannot be determined on a simple dimensional basis.

A simple way to modify the K41 consists in assuming that the energy dissipation is uniformly distributed on homogeneous fractal with dimension $D_F < 3$. This implies $\delta v_\ell(\mathbf{x}) \sim \ell^h$ with $h = (D_F - 2)/3$ for $\mathbf{x}$ on the fractal and $\delta v_\ell(\mathbf{x})$ non-singular otherwise. This assumption (called absolute curdling or β-model) gives

$$\zeta_p = \frac{D_F - 2}{3} p + (3 - D_F). \tag{5}$$

Such a prediction, with $D_F \simeq 2.83$, is in fair agreement with the experimental data for small values of p, but higher order scaling exponents give a clear indication of a nonlinear behavior in p.

The multifractal model of turbulence [1, 13, 19] assumes that the velocity has a local scale-invariance, i.e. there is not a unique scaling exponent h such that $\delta v_\ell \sim \ell^h$, but a continuous spectrum of exponents, each of which belonging to a given fractal set. In other words, in the inertial range one has

$$\delta v_\ell(\mathbf{x}) \sim \ell^h, \tag{6}$$

if $\mathbf{x} \in S_h$, and S_h is a fractal set with dimension $D(h)$ and $h \in (h_{\min}, h_{\max})$. The probability to observe a given scaling exponent h at the scale ℓ is $P_\ell(h) \sim \ell^{3-D(h)}$, and therefore one has

$$S_p(\ell) = \langle |\delta v_\ell|^p \rangle \sim \int_{h_{\min}}^{h_{\max}} \ell^{hp} \ell^{3-D(h)} \, \mathrm{d}h \sim \ell^{\zeta_p}. \tag{7}$$

For $\ell \ll 1$, a steepest descent estimation gives

$$\zeta_p = \min_h \{hp + 3 - D(h)\} = h^* p + 3 - D(h^*), \tag{8}$$

where $h^* = h^*(p)$ is the solution of the equation $D'(h^*(p)) = p$. The Kolmogorov '4/5' law (4) imposes $\zeta_3 = 1$ which implies that

$$D(h) \leqslant 3h + 2, \tag{9}$$

with the equality realized by $h^*(3)$. The Kolmogorov similarity theory corresponds to the case of only one singularity exponent $h = 1/3$ with $D(h = 1/3) = 3$.

Of course the computation of $D(h)$, or equivalently ζ_p, from the NSE is not at present an attainable goal. A first step is a phenomenological approach using multiplicative processes. Let us briefly remind the so-called random β-model [2]. This model describes the energy cascade in real space looking at eddies of size $\ell_n = 2^{-n}L$, with L the length at which the energy is injected. At the nth step of the cascade a mother eddy of size ℓ_n splits into daughter eddies of size ℓ_{n+1}, and the daughter eddies cover a fraction β_j ($0 < \beta_j < 1$) of the mother volume. As a consequence of the fact that the energy transfer is constant throughout the cascade one has for the velocity differences $v_n = \delta v_{\ell_n}$ on the scale ℓ_n is non-negligible only on a fraction of volume $\prod_j \beta_j$, and is given by

$$v_n = v_0 \ell_n^{1/3} \prod_{j=1}^n \beta_j^{-1/3}, \tag{10}$$

where β_js are independent, identically distributed random variables. Phenomenological arguments suggest that $\beta_j = 1$ with probability x and $\beta_j = B = 2^{-(1-3h_{\min})}$ with probability $1 - x$. The above multiplicative process generates a two-scale Cantor set, which is a rather common structure in chaotic systems. The scaling exponents are

$$\zeta_p = \frac{p}{3} - \ln_2[x + (1 - x)B^{1-p/3}] \tag{11}$$

corresponding to

$$D(h) = 3 + \left(3h - 1\right)\left[1 + \ln_2\left(\frac{1 - 3h}{1 - x}\right)\right] + 3h \ln_2\left(\frac{x}{3h}\right). \tag{12}$$

The two limit cases are $x = 1$, i.e. the K41, and $x = 0$ which is the β-model with $D_F = 2 + 3h_{\min}$. Using $x = 7/8$, $h_{\min} = 0$ (i.e. $B = 1/2$), one has a good fit for the ζ_p of the experimental data at high Reynolds numbers.

Of course it is not so astonishing to find a model to fit the experimental data. Indeed, there are now many phenomenological models for $D(h)$ which provide scaling exponents in agreement with experimental data. A popular one is the so-called She–Lévêque model [20] which is reproduced by the multifractal model with

$$D(h) = 1 + \frac{2\beta - 3h - 1}{\ln \beta}\left[1 - \ln\left(\frac{2\beta - 1 - 3h}{2 \ln \beta}\right)\right]$$

and gives for the scaling exponents

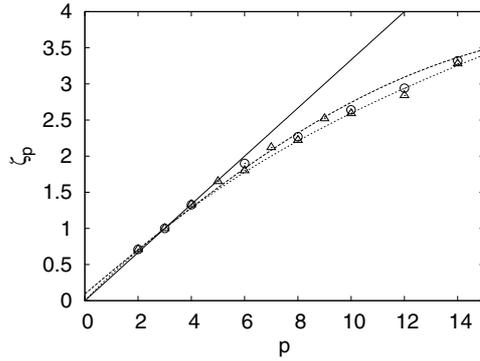$$\zeta_p = \frac{2\beta - 1}{3}p + 2(1 - \beta^{p/3}) \tag{13}$$

Figure 1. Structure function scaling exponents ζ_p plotted versus p. Circles and triangles correspond to the data of Anselmet *et al* [18]. The solid line corresponds to Kolmogorov scaling $p/3$; the dashed line is the random β-model prediction (11) with $B = 1/2$ and $x = 7/8$; the dotted line is the She–Lévêque prediction (13) with $\beta = 2/3$.

which are close to the experimental data for $\beta = 2/3$. Another important model, which was introduced by Kolmogorov himself without reference to the multifractal model, is the log-normal model which will be discussed in section 2.2.

The relevance, and the success, of the multifractal approach is in the possibility to predict, and test, nontrivial statistical features, e.g. the probability density function (PDF) of the velocity gradient, the existence of an intermediate dissipative range and precise scaling for Lagrangian quantities. Once $D(h)$ is obtained by a fit of the experimental data, e.g. from the ζ_p, then all the predictions obtained in the multifractal model framework must be verified without additional free parameters.

2.2. Relation between the original multifractal model and the $f(\alpha)$ versus α

The multifractal model for the FDT previously discussed is linked to the so-called $f(\alpha)$ versus α description of the singular measures (e.g. in chaotic attractors) [12, 14, 21]. In order to show this connection let us recall the Kolmogorov revised theory [5] (called K62) stating that the velocity increments δv_ℓ scales as $(\epsilon_\ell \ell)^{1/3}$, where ϵ_ℓ is the energy dissipation space-averaged over a cube of edge ℓ. Let us introduce the measure $\mu(\mathbf{x}) = \epsilon(\mathbf{x})/\bar{\epsilon}$, a partition of non-overlapping cells of size ℓ and the coarse graining probability

$$P_i(\ell) = \int_{\Lambda_\ell(\mathbf{x})} d\mu(\mathbf{y})$$

where $\Lambda_l(\mathbf{x}_i)$ is a cube of edge ℓ centered in $\mathbf{x}_i$, of course $\epsilon_\ell \sim \ell^{-3} P(\ell)$. Denoting with α the scaling exponent of P_ℓ and with $f(\alpha)$ the fractal dimension of the subfractal with a scaling exponent α, we can introduce the Renyi dimensions d_p:

$$\sum_i P_i(\ell)^p \sim \ell^{(p-1)d_p},$$

where the sum is over the non-empty boxes. A simple computation gives

$$(p - 1)d_p = \min_\alpha [p\alpha - f(\alpha)].$$

Noting that $\left\langle \epsilon_\ell^p \right\rangle = \ell^3 \sum \epsilon_\ell^p$, we have

$$\left\langle \epsilon_\ell^p \right\rangle \sim \ell^{(p-1)(d_p-3)},$$

therefore one has the correspondence

$$h \leftrightarrow \frac{\alpha - 2}{3}, \qquad D(h) \leftrightarrow f(\alpha), \qquad \zeta_p = \frac{p}{3} + \left(\frac{p}{3} - 1\right)\left(d_{\frac{p}{3}} - 3\right).$$

Of course the result $\zeta_3 = 1$, once assumed $\delta v \sim (\epsilon_\ell \ell)^{1/3}$, holds for any $f(\alpha)$. Let us note that the log-normal theory K62 where

$$\zeta_p = \frac{p}{3} + \frac{\mu}{18} p(3 - p)$$

is a special case of the multifractal model, where there are no restrictions on the values of h and $D(h)$ is a parabola with a maximum at $D_F = 3$:

$$D(h) = -\frac{9}{2\mu} h^2 + \frac{3}{2}(2 + \mu)h - \frac{4 - 20\mu + \mu^2}{8\mu}$$

and the parameter μ is determined by the fluctuation of $\ln \epsilon_\ell$.

2.3. A technical remark on multifractality

To obtain the scaling behavior of $S_p(\ell) \sim (\ell/L)^{\zeta_p}$ given by (7) with ζ_p obtained from (8), one has to assume that the exponent $ph + 3 - D(h)$ has a minimum, ζ_p, which is a function of h, and that such an exponent behaves quadratically with h in the vicinity of the minimum. This is the basic assumption to apply the Laplace method of steepest descent [22]. The point we would like to recall here is that, for small separations, ℓ, it is true that $S_p(\ell) \sim (\ell/L)^{\zeta_p}$ but with a logarithmic prefactor:

$$S_p(\ell) \sim \left[-\ln\left(\frac{\ell}{L}\right)\right]^{-1/2} \left(\frac{\ell}{L}\right)^{\zeta_p}. \tag{14}$$

Such a prefactor is usually not considered in the naive application of the Laplace method leading to (7). The presence of such logarithmic correction, if present, would clearly invalidate the 4/5th law (4), one of the very few exact results in fully developed turbulence.

The question on whether such logarithmic correction is likely has quantitatively been addressed by Frisch *et al* [23]. There, exploiting the refined large-deviations theory, the authors were able to explain in which way the logarithmic contribution cancels out thus giving rise to a prediction fully compatible with the naive (*a priori* unjustified) procedure to extract the scaling behavior (7). The key point is that the leading-order large deviation result for the probability $P_\ell(h)$ to be within a distance ℓ of the set carrying singularities of scaling exponent between h and $h + dh$,

$$P_\ell(h) \sim \left(\frac{\ell}{L}\right)^{3 - D(h)}, \tag{15}$$

must be generalized to take into account the next subleading order. In doing so, as a result one obtains [23]

$$P_\ell(h) \sim \left(\frac{\ell}{L}\right)^{3 - D(h)} \left[-\ln \frac{\ell}{L}\right]^{1/2}, \tag{16}$$

which contains subleading logarithmic correction. It is worth observing that despite the multiplicative character of the logarithmic correction one speaks of 'subleading correction'. This is justified by the fact that the correct statement of the large-deviations leading-order result involves the logarithm of the probability divided by the logarithm of the scale. The correction is then a subleading additive term.

Once expression (16) is plugged in the integral

$$S_p(\ell) \sim \int dh \, P_\ell(h) \left(\frac{\ell}{L} \right)^{ph} \tag{17}$$

and the saddle point estimation is carried out according to [22], logarithms disappear and the expected 4/5th law emerges.

It is worth mentioning that the presence of a square root of a logarithm correction in the multifractal probability density had already been proposed by [24] on the basis of a normalization requirement. In that paper, the authors observed that without such a correction the singularity spectrum $f(\alpha)$ comes out wrong; they also pointed out that a similar correction has been proposed by [25] in connection with the measurement of generalized Renyi dimensions.

3. Implications of multifractality on Eulerian features

At first we note that a consequence of the presence of the intermittency the Kolmogorov scale does not take a unique value. The local dissipative scale ℓ_D is determined by imposing the effective Reynolds number to be of order unity:

$$Re(\ell_D) = \frac{\delta v_D \ell_D}{\nu} \sim 1, \tag{18}$$

therefore the dependence of ℓ_D on h is thus

$$\ell_D(h) \sim L Re^{-\frac{1}{1+h}}, \tag{19}$$

where $Re = Re(L)$ is the large-scale Reynolds number [26].

In this section we will show that the fluctuations of the dissipative scale, due to the intermittency in the turbulent cascade, is relevant of the statistical features of the velocity differences and velocity gradient, and in addition it implies the existence of an intermediate region between the inertial and dissipative range [27].

3.1. The PDF of the velocity differences and velocity gradient

Let us denote by s the longitudinal velocity gradient. Such a quantity can immediately be expressed in terms of the singularity exponents h as

$$|s| \sim \frac{\delta v_{\ell_D}}{\ell_D} = v_0 \ell_D^{h-1} = v_0^{\frac{2}{1+h}} \nu^{\frac{h-1}{h+1}}, \tag{20}$$

where we used the fact that $\delta v_\ell \sim v_0 l^h$ from (6) and we have exploited (19). From (20) we realize that we can easily express the PDF of s (for a fixed h), $P_h(s)$, in terms of the PDF, $\Pi(V_0)$, of the large-scale velocity differences V_0, with $v_0 \equiv |V_0|$. The latter PDF is indeed known to be accurately described by the Gaussian distribution [28]. The link between the two PDFs is given by the standard relation

$$P_h(s) = \Pi(V_0) \left| \frac{dV_0}{ds} \right| \tag{21}$$

from which one immediately gets

$$P_h(s) \sim \left(\frac{\nu}{|s|} \right)^{\frac{1-h}{2}} e^{-\frac{\nu^{1-h}|s|^{1+h}}{2\langle V_0^2 \rangle}}. \tag{22}$$

The K41 theory and the β-model correspond to $h = 1/3$ and $h = (D_F - 2)/3$, respectively. In both cases, a stretched exponential form for the PDF is predicted with an exponent, $1 + h$,

larger than 1. Experimental data (see, e.g. [29, 30]) are not consistent with such a prediction being actually compatible with a stretched exponent whose value is smaller than 1.

The multifractal description has thus to be exploited to capture those experimental evidences. To do that we recall expression (10) for the random β-model

$$v_n = v_0 \ell_n^{1/3} \prod_{j=1}^{n} \beta_j^{-1/3} \tag{23}$$

from which the probability distribution of the velocity increments v_n reads

$$P(v_n) = \int \Pi(V_0)\, \mathrm{d}V_0 \int \delta \left(v_n - v_0 l_n^{1/3} \prod_{i=1}^{n} \beta_i^{-1/3} \right) \prod_{j=1}^{n} \beta_i \mu(\beta_i)\, \mathrm{d}\beta_i. \tag{24}$$

Here, $\mu(\beta_i)$ is the probability density of β_i s assumed to be of the form

$$\mu(\beta_i) = x\delta(\beta_i - 1) + (1-x)\delta(\beta_i - B) \tag{25}$$

with $B = 2^{-(1-3h_{\min})}$.

Since β_is are identically distributed, the above integral becomes

$$P(v_n) = \sum_{K=0}^{n} \binom{n}{K} x^{n-K} (1-x)^K B^{4K/3} l_n^{-1/3} \, \mathrm{e}^{-CB^{2K/3} l_n^{-2/3} v_n^2} \tag{26}$$

with $C \equiv (2\langle V_0^2 \rangle)^{-1}$. It is easy to see [31] the passage of the above PDF from a Gaussian form at large scales (small n) to an exponential-like form at small scales (large n).

To obtain the gradient PDF from (26) it is sufficient to stop the sum at $n = N$ such that $v_N l_N / v = 1$. This is equivalent to say

$$l_N^2 = 2^{-2N} \sim \frac{\nu}{s} \qquad \text{or} \qquad N = \frac{\ln \frac{s}{\nu}}{2 \ln 2}. \tag{27}$$

By noting that $B^{2N} = (\nu/s)^{1-3h_{\min}}$ the resulting gradient PDF reads

$$P(s) \sim \sum_{K=0}^{N} \binom{N}{K} x^{N-K} (1-x)^K \left(\frac{\nu}{|s|} \right)^{(1+2q)/3} \mathrm{e}^{-C\nu^{(2+q)/3}|s|^{(4-q)/3}}, \tag{28}$$

where $q \equiv K(1 - 3h_{\min})/N$. The K41 prediction corresponds to considering only the term $K = 0$ with $x = 1$.

We already discussed that $x = 7/8$ and $h_{\min} = 0$ provide a good fit for the scaling exponents ζ_p of the structure functions in the limit of high Reynolds numbers. The same parameters give a PDF behavior in good agreement with the available experimental data (see [31] and figure 2).

3.2. Intermediate dissipative range

Now let us show that as a consequence of the fluctuations of the dissipative scale one has the existence of an intermediate region (the intermediate dissipative range, IDR) between the inertial and dissipative range [27]. The presence of fluctuations of ℓ_D, see (19), modifies the evaluation of the structure functions (7): for a given ℓ, the saddle point evaluation remains unchanged if, for the selected exponent $h^*(p)$, one has $\ell_D(h^*(p)) < \ell$. If, in contrast, the selected exponent is such that $\ell_D(h^*(p)) > \ell$ the saddle point evaluation is not consistent, because at scale ℓ the power-law scaling (6) is no longer valid. In this intermediate dissipation range, the integral in (7) is dominated by the smallest acceptable scaling exponent $h(\ell)$ given by inverting (19), and the structure function of order p a pseudo-algebraic behavior, i.e. a
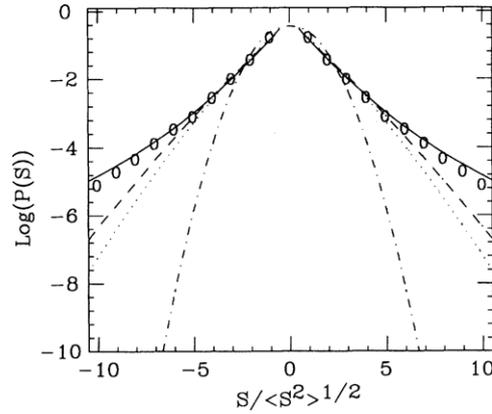
Figure 2. Log-linear plot of the PDF of velocity gradients s rescaled with the rms value. Points represent experimental data from [30], solid line is the multifractal prediction with the random β-model, dotted and dashed lines represent the K41 and β-model results, respectively.

power law with exponent $ph(\ell) + 3 - D(h(\ell))$ which depends on the scale ℓ. Taking into account the fluctuations of the dissipative range [27], one has for the structure functions

$$S_p(\ell) \sim \begin{cases} \ell^{\zeta_p} & \text{if} \quad \ell_D(h^*(p)) < \ell \\ \ell^{h(\ell)p+3-D(h(\ell))} & \text{if} \quad \ell_D(h_{\min}) < \ell < \ell_D(h^*(p)). \end{cases} \tag{29}$$

A simple calculation [27, 13] shows that it is possible to find a universal description valid both in the inertial and in the intermediate dissipative ranges. Let us discuss this point for the energy spectrum $E(k)$. Introducing the rescaled variables

$$F(\theta) = \frac{\ln E(k)}{\ln Re} \qquad \text{and} \qquad \theta = \frac{\ln k}{\ln Re}, \tag{30}$$

one obtains the following behavior:

$$F(\theta) = \begin{cases} -(1 + \zeta_2)\theta & \text{for} \quad \theta < \dfrac{1}{1 + h^*(2)} \\ -2 - 2\theta + \theta D(\theta^{-1} - 1) & \text{for} \quad \dfrac{1}{1 + h^*(2)} < \theta < \dfrac{1}{1 + h_{\min}}. \end{cases} \tag{31}$$

The prediction of the multifractal model is that $\ln E(k)/\ln Re$ is a universal function of $\ln k/\ln Re$. This is in contrast with the usual scaling hypothesis according to which $\ln E(k)$ should be a universal function of $\ln(k/k_D)$). The multifractal universality has been tested by collapsing energy spectra obtained from turbulent flow in a wide range of Re [32], see also [33].

3.3. Exit times for turbulent signals and the IDR

In the following we will discuss a method alternative to the study of the structure functions which allows for a deeper understanding of the IDR.

Basically, in typical experiments one is forced to analyze the one-dimensional string of data $v(t)$, e.g. the output of hot-wire anemometer, and the Taylor frozen-turbulence hypothesis is used to bridge measurements in space with measurements in time. As a function of time increment, τ, structure functions assume the form: $S_p(\tau) = \langle [(v(t + \tau) - v(t)]^p \rangle$. In the

inertial range, $\tau_D \ll \tau \ll T_0$ (where $T_0 = L_0/V_0$, and the dissipative time, $\tau_D = \ell_D/V_0$), the structure functions develop an anomalous scaling behavior: $S_p(\tau) \sim \tau^{\zeta_p}$, where $\tau \sim \ell/V_0$.

The main idea, which can be applied both to experimental and synthetic data, is to take a time sequence $v(t)$, and to analyze the statistical properties of the exit times from a set of defined velocity thresholds. More precisely, given a reference initial time t_0 with velocity $v(t_0)$, we define $\tau(\delta v)$ as the first time necessary to have an absolute variation equal to δv in the velocity data, i.e. $|v(t_0) - v(t_0 + \tau(\delta v))| = \delta v$. By scanning the whole time series we recover the probability density functions of $\tau(\delta v)$ at varying δv from the typical large-scale values down to the smallest dissipative values. Positive moments of $\tau(\delta v)$ are dominated by events with a smooth velocity field, i.e. laminar bursts in the turbulent cascade. Let us define the inverse structure functions (Inverse-SF) as [33, 34]

$$\Sigma_p(\delta v) \equiv \langle \tau^p(\delta v) \rangle. \tag{32}$$

It is necessary to perform weighted average over the time-statistics in a weighted way. This is due to the fact that by looking at the exit-time statistics we are not sampling the time-series uniformly, i.e. the higher the value of $\tau(\delta v)$ is, the longer it remains detectable in the time series.

It is possible to show [35] that the sequential time average of any observable, $\mathcal{A}$, based on exit-time statistics, $\langle \mathcal{A} \rangle_e$, is connected to the uniformly-in-time multifractal average by the relation

$$\langle A \rangle = \frac{\langle A\tau \rangle_e}{\langle \tau \rangle_e}. \tag{33}$$

For $\mathcal{A} = \tau^p(\delta v)$ the above relations becomes

$$\langle \tau^p(\delta v) \rangle = \frac{\langle \tau^{p+1} \rangle_e}{\langle \tau \rangle_e}. \tag{34}$$

According to the multifractal description we assume that for velocity thresholds corresponding to inertial range values of the velocity differences the following dimensional relation is valid:

$$\delta_\tau v \sim \tau^h \rightarrow \tau(\delta v) \sim \delta v^{1/h},$$

and the probability to observe a value τ for the exit time is given by inverting the multifractal probability, i.e. $P(\tau \sim \delta v^{1/h}) \sim \delta v^{[3-D(h)]/h}$. With this ansatz in the inertial range one has

$$\Sigma_p(\delta v) \sim \int_{h_{min}}^{h_{max}} dh\, \delta v^{[p+3-D(h)]/h} \sim \delta v^{\chi_p}, \tag{35}$$

where with the Laplace method one obtains

$$\chi_p = \min_h \{[p + 3 - D(h)]/h\}. \tag{36}$$

Now let us consider the IDR properties.

For each p, the saddle point evaluation selects a particular $h = h_s(p)$ where the minimum is reached. Let us also remark that from (35) we have an estimate for the minimum value assumed by the velocity in the inertial range given a certain singularity h: $v_m(h) = \delta_{\tau_d(h)} v \sim v^{h/(1+h)}$. Therefore, the smallest velocity value at which the scaling (35) still holds depends on both ν and h. Namely, $\delta v_m(p) \sim v^{h_s(p)/1+h_s(p)}$. The most important consequence is that for $\delta v < \delta v_m(p)$ the integral (35) is not any more dominated by the saddle point value but by the maximum h value still dynamically alive at that velocity difference, $1/h(\delta v) = -1 - \log(v)/\log(\delta v)$. This leads for $\delta v < \delta v_m(p)$ to a pseudo-algebraic law:

$$\Sigma_p(\delta v) \sim \delta v^{[p + 3 - D(h(\delta v))]/h(\delta v)}. \tag{37}$$
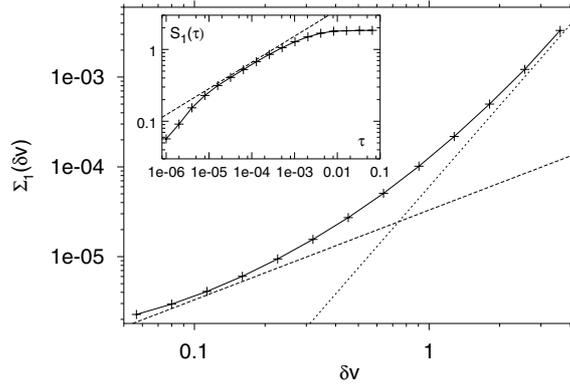
Figure 3. Inverse structure functions $\Sigma_1(\delta v)$. The straight lines show the dissipative range behavior (dashed) $\Sigma_1(\delta v) \sim \delta v$, and the inertial range non-intermittent behavior (dotted) $\Sigma_1(\delta v) \sim (\delta v)^3$. The inset shows the direct structure function $S_1(\tau)$ with the superimposed intermittent slope $\zeta_1 = 0.39$.

The presence of this p-dependent velocity range, intermediate between the inertial range, $\Sigma_p(\delta v) \sim \delta v^{\chi_p}$, and the dissipative scaling, $\Sigma_p(\delta v) \sim \delta v^p$, is the IDR signature.

In figure 3 we show $\Sigma_1(\delta v)$ evaluated on a string of high-Reynolds number experimental data as a function of the available range of velocity thresholds δv. This data set has been measured in a wind tunnel at $Re_\lambda \sim 2000$. One can see that the scaling is very poor. On the other hand (the inset of figure 3), the scaling behavior of the direct structure functions $\langle|\delta v(\tau)|\rangle \sim \tau^{\zeta_1}$ is quite clear in a wide range of scales. This is a clear evidence of IDR's contamination into the whole range of available velocity values for the Inverse-SF cases.

Now let us go back to the statistical properties of the IDR. In order to study this question we have smoothed the stochastic synthetic field, $v(t)$ (see the appendix) by performing a running-time average over a time-window, δT. Then we compare Inverse-SF obtained for different Reynolds numbers, i.e. for different dissipative cut-off: $Re \sim \delta T^{-4/3}$.

Expression (37) predicts the possibility to obtain a data collapse of all curves with different Reynolds numbers by rescaling the Inverse-SF as follows [27, 36]:

$$-\ln(\Sigma_p(\delta v))/\ln(\delta T/\delta T_0) \qquad \text{versus} \qquad -\ln(\delta v/U)/\ln(\delta T/\delta T_0), \qquad (38)$$

where U and δT_0 are adjustable dimensional parameters.

Figure 4 shows the rescaling (38) of the Inverse-SF, $\Sigma_1(\delta v)$, both for the synthetic field at different Reynolds numbers and for the experimental signals. As it is possible to see, the data collapse is very good. This is a clear evidence that the poor scaling range observed in figure 4 for the experimental signal can be explained as the signature of the IDR.

4. The relation between Eulerian and Lagrangian statistics

A problem of great interest concerns the study of the spatial and temporal structure of the so-called passive fields, indicating by this term quantities transported by the flow without affecting the velocity field. The paradigmatic equation for the evolution of a passive scalar field $\theta(\mathbf{x}, t)$ advected by a velocity field $\mathbf{v}(\mathbf{x}, t)$ is [37]

$$\partial_t \theta + \nabla \cdot (\mathbf{v}\theta) = \chi \nabla^2 \theta \qquad (39)$$

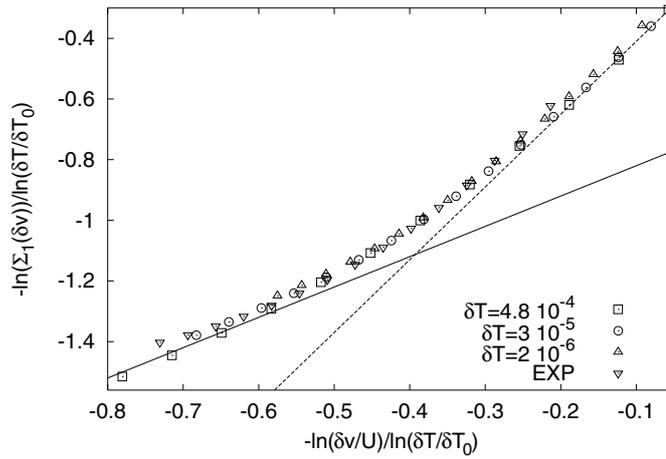where χ is the molecular diffusion coefficient.

Figure 4. Data collapse of the Inverse-SF, $\Sigma_1(\delta v)$, obtained by the rescaling (38) for the smoothed synthetic signals (with time windows: $\delta T = 4.8 \times 10^{-4}, 3 \times 10^{-5}, 2 \times 10^{-6}$) and the experimental data (EXP). The two straight lines have the dissipative (solid line) and the inertial range (dashed) slope.

Problem (39) can be studied through two equivalent approaches, both due to Euler [38]. The first, referred to as 'Eulerian', deals at any time with the field θ in the space domain covered by the fluid; the second considers the time evolution of trajectories of each fluid particle and is called 'Lagrangian'.

The motion of a fluid particle is determined by the differential equation

$$\frac{d\mathbf{x}}{dt} = \mathbf{v}(\mathbf{x}, t) \tag{40}$$

which also describes the motion of test particles, for example a powder embedded in the fluid, provided that the particles are neutral and small enough not to perturb the velocity field, although large enough not to perform a Brownian motion. Particles of this type are commonly used for flow visualization in fluid mechanics experiments [39]. We remark that the complete equation for the motion of a material particle in a fluid when density and volume effects are taken into account can be rather complicated [40, 41].

The Lagrangian equation of motion (40) formally represents a dynamical system in the phase-space of physical coordinates. By very general considerations, it is now well established that even in regular velocity field the motion of fluid particles can be very irregular [42, 43]. In this case initially nearby trajectories diverge exponentially and one speaks of *Lagrangian chaos* or *chaotic advection*. In general, chaotic behaviors can arise in two-dimensional flow only for time-dependent velocity fields, while it can be present even for stationary velocity fields in three dimensions.

If $\chi = 0$, it is easy to realize that (39) is equivalent to (40). Indeed, we can write

$$\theta(\mathbf{x}, t) = \theta(T^{-t}\mathbf{x}, 0), \tag{41}$$

where T is the formal evolution operator of (40): $\mathbf{x}(t) = T^t\mathbf{x}(0)$.

Taking into account the molecular diffusion χ, (39) is the Fokker–Planck equation of the Langevin equation [44]

$$\frac{d\mathbf{x}}{dt} = \mathbf{v}(\mathbf{x}, t) + \eta(t), \tag{42}$$

where η is a Gaussian process with zero mean and variance

$$\langle \eta_i(t)\eta_j(t')\rangle = 2\chi\delta_{ij}\delta(t-t'). \tag{43}$$

The dynamical system (40) becomes conservative in the phase-space in the case of an incompressible velocity field for which

$$\nabla \cdot \mathbf{v} = 0. \tag{44}$$

In two dimensions, $\mathbf{x} = (x_1, x_2)$, the constraint (44) is automatically satisfied by introducing the stream function $\psi(\mathbf{x}, t)$

$$v_1 = \frac{\partial \psi}{\partial x_2}, \qquad v_2 = -\frac{\partial \psi}{\partial x_1} \tag{45}$$

and the evolution equation becomes

$$\frac{\mathrm{d}x_1}{\mathrm{d}t} = \frac{\partial \psi}{\partial x_2}, \qquad \frac{\mathrm{d}x_2}{\mathrm{d}t} = -\frac{\partial \psi}{\partial x_1}; \tag{46}$$

i.e. formally a Hamiltonian system with the Hamiltonian given by the stream function, ψ.

The presence of Lagrangian chaos in regular flows is a remarkable example of the fact that, in general, it is very difficult to relate the Lagrangian and Eulerian statistics. For example, from very complicated trajectories of buoys one cannot infer the time-dependent circulation of the sea. In the following sections, we will see that in the case of fully developed turbulence the disordered nature of the flow makes this connection partially possible at a statistical level.

The equation of motion (40) shows that the trajectory of a single particle is not Galilean invariant, i.e. invariant with respect to the addition of a mean velocity. The most general Galilean invariant statistics, which is ruled by a small-scale velocity fluctuation, is given by multi-particle, multi-time correlations for which we could expect universal features. In the following we will consider separately the two most studied statistics: single-particle two-time velocity differences and two-particle single-time relative dispersion.

4.1. Single-particle statistics: multifractal description of Lagrangian velocity differences

The simplest Galilean invariant Lagrangian quantity is the single-particle velocity increment $\delta\mathbf{v}(t) = \mathbf{v}(t_0 + t) - \mathbf{v}(t_0)$, where $\mathbf{v}(t) = \mathbf{v}(\mathbf{x}(t), t)$ denotes the Lagrangian velocity of the particle at $\mathbf{x}(t)$ and the independence on t_0 is a consequence of the stationarity of the flow. Dimensional analysis in fully developed turbulence predicts [15, 45]

$$\langle \delta v_i(t)\delta v_j(t)\rangle = C_0 \bar{\varepsilon} t \delta_{ij}, \tag{47}$$

where $\bar{\varepsilon}$ is the mean energy dissipation and C_0 is a numerical constant. The remarkable coincidence that the variance of $\delta\mathbf{v}(t)$ grows linearly with time is the physical basis on which stochastic models of particle dispersion are based. It is important to recall that the 'diffusive' nature of (47) is purely incidental: it is a direct consequence of Kolmogorov scaling in the inertial range of turbulence and is not directly related to a diffusive process (i.e. there is no decorrelation justifying the applicability of central limit theorem).

Let us briefly recall the argument leading to the scaling in (47). We can think at the velocity $v(t)$ advecting the Lagrangian trajectory as the superposition of the different velocity contributions coming from turbulent eddies (which also move with the same velocity of the Lagrangian trajectory). After a time t the components associated with the smaller (and faster) eddies, below a certain scale ℓ, are decorrelated and thus at the leading order one has $\delta v(t) \simeq \delta v(\ell)$. Within Kolmogorov scaling, the velocity fluctuation at the scale ℓ is given by $\delta v(\ell) \sim V_0(\ell/L)^{1/3}$, where V_0 represents the typical velocity at the largest scale L. The
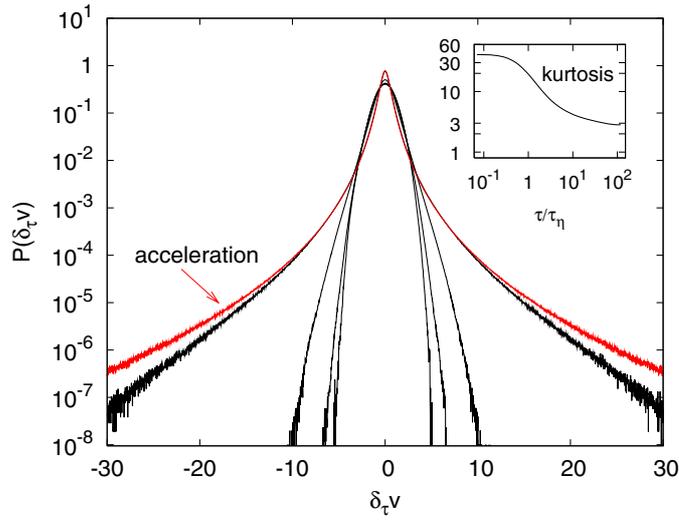
Figure 5. Probability density functions of velocity increments for a numerical simulation at $R_\lambda = 284$. Curves refer to time increments $t = (97, 24, 6, 0.7)\tau_D$ from inside to outside (and to the acceleration). In the inset kurtosis $\langle \delta v(t)^4 \rangle / \langle \delta v(t)^2 \rangle^2$ as a function of time delay is shown. Figure from [49].

correlation time of $\delta v(\ell)$ scales as $\tau(\ell) \sim \tau_0 (\ell/L)^{2/3}$ and thus one obtains the scaling in (47) with $\varepsilon = V_0^2 / \tau_0$.

Equation (47) can be generalized to higher order moments with the introduction of a set of temporal scaling exponents ξ_p:

$$\langle \delta v(t)^p \rangle \sim V_0^p (t/\tau_0)^{\xi_p}. \tag{48}$$

The dimensional estimation sketched above gives the prediction $\xi_p = p/2$, but one may expect corrections to the dimensional scaling in the presence of intermittency.

A generalization of the above results which takes into account intermittency corrections can be easily developed by using the multifractal model [46, 47]. The dimensional argument is repeated for the local scaling exponent h, giving $\delta v(t) \sim V_0 (t/\tau_0)^{h/(1-h)}$. Integrating over the h distribution one ends with

$$\langle \delta v(t)^p \rangle \sim V_0^p \int dh \left(\frac{t}{\tau_0} \right)^{[ph - D(h) + 3]/(1-h)}, \tag{49}$$

where $D(h)$ is the Eulerian fractal dimension (i.e. related to the Eulerian structure function scaling exponents by $\zeta(q) = \min_h [qh - D(h) + 3]$). In the limit $t/\tau_0 \to 0$, the integral can be estimated by a steepest descent argument giving the prediction

$$\xi_p = \min_h \left[\frac{ph - D(h) + 3}{1 - h} \right]. \tag{50}$$

The standard inequality in the multifractal model $D(h) \leqslant 3h + 2$ implies for (50) that even in the presence of intermittency $\xi_2 = 1$. Physically, this is a consequence of the fact that energy dissipation is raised to the first power, in (47).

Experimental results [48] have shown that even at large Reynolds number the scaling (47) is not clearly observed. Therefore, the dimensionless constant C_0 is known with large uncertainty, if compared with the Kolmogorov constant.
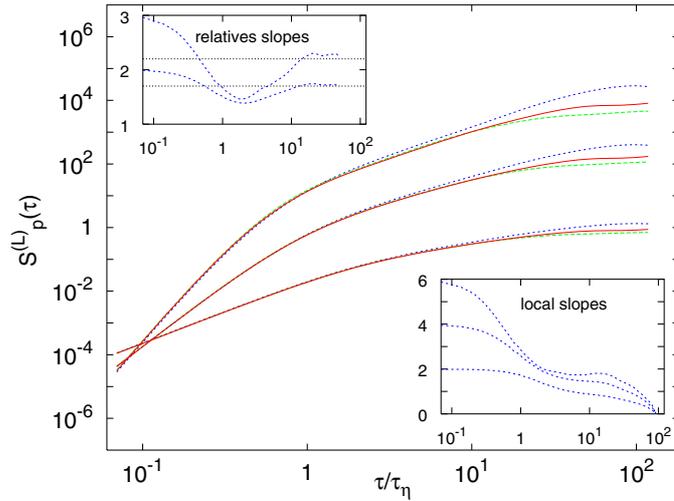
Figure 6. Log–log plot of Lagrangian structure functions of order 2, 4 and 6 (bottom to top) for the three components of the velocity obtained from DNS at $R_\lambda = 284$. Small differences between the components are observed at large delays as a consequence of small anisotropies at large scales. In the insets the local slopes (bottom right) and relative slopes (top left) are shown for the x-component. Relative slopes are defined as $dS_p(t)/dS_2(t)$ for $p = 4, 6$. The horizontal lines represent the multifractal prediction. Figure from [49].

Intermittency in Lagrangian velocity differences is evident by looking at the PDF of $\delta v(t)$ at different time lags, as shown in figure 5. For large time delays the PDF are close to Gaussian while decreasing t they develop larger and larger tails, implying the breakdown of self-similarity.

Higher order Lagrangian structure functions are shown in figure 6 for a set of direct numerical simulations at $R_\lambda = 284$ [50, 49]. Despite the apparent scaling observed in the log–log plot, the computation of local slopes does not give a definite value of scaling exponents. Assuming $\xi_2 = 1$ as predicted by (50), one can measure the *relative* scaling exponent ξ_p/ξ_2 by using the so-called extended self-similarity procedure [51]. As shown in the inset of figure 6, we observe a well-defined scaling in the range of separations $10\tau_D \leqslant \tau \leqslant 50\tau_D$. The values of the relative exponents estimated with this method, $\xi_4/\xi_2 = 1.7 \pm 0.05$, $\xi_5/\xi_2 = 2.0 \pm 0.05$, $\xi_6/\xi_2 = 2.2 \pm 0.07$, are in good agreement with those predicted by the multifractal model (50).

The multifractal prediction (50) has also been checked in the simplified Lagrangian model based on the shell model of turbulence [47].

5. Lagrangian acceleration statistics

Acceleration in fully developed turbulence is an extremely intermittent quantity which displays fluctuations up to 80 times its root mean square [52]. These extreme events generate very large tails in the PDF of acceleration which are therefore expected to be very far from Gaussian.

We remark that even within non-intermittent Kolmogorov scaling, acceleration PDF is expected to be non-Gaussian. Indeed acceleration can be estimated from velocity fluctuations at the Kolmogorov scale as

$$a = \frac{\delta v(\tau_D)}{\tau_D}, \tag{51}$$

15

where $\tau_D = \eta/\delta v(\eta)$ and the Kolmogorov scale η is given by the condition $\eta \delta v(\eta)/\nu = 1$. By assuming the scaling $\delta v(\ell) \simeq V_0(\ell/L)^h$ (with $h = 1/3$ for Kolmogorov scaling), one obtains

$$\frac{\eta}{L} \sim \left(\frac{V_0 L}{\nu}\right)^{-\frac{1}{1+h}} \tag{52}$$

and therefore

$$a = \frac{V_0^2}{L} \left(\frac{V_0 L}{\nu}\right)^{\frac{1-2h}{1+h}}. \tag{53}$$

Assuming a Gaussian distribution for the large-scale velocity fluctuations V_0 (which is, as already observed, consistent with many experimental and numerical observations), and taking $h = 1/3$, one obtains for the PDF of a a stretched exponential tail $p(a) \sim \exp(-Ca^{8/9})$.

In the presence of intermittency, the above argument has to be modified by taking into account the fluctuations of scaling exponent. In the recent years, several models have been proposed for describing turbulent acceleration statistics, on the basis of different physical ingredients. In the following we want to show that the multifractal model of turbulence, when extended to describe fluctuation at the dissipative scale, is able to predict the PDF of acceleration observed in simulations and experiments with high accuracy [53]. Moreover, as in the case of Lagrangian structure functions, the model does not require the introduction of new parameters, a part of the set of Eulerian scaling exponents. In this sense, the multifractal model become a *predictive* model for Lagrangian statistics.

The introduction of intermittency in the above argument is simply obtained by weighting (53) with both the distribution of V_0 (still assumed Gaussian, as intermittency is not expected to affect large-scale statistics) and the distribution of scaling exponent h which can be rewritten as

$$p(h) \sim \left(\frac{\eta}{L}\right)^{3-D(h)} \sim \left(\frac{V_0 L}{\nu}\right)^{\frac{D(h)-3}{1+h}}. \tag{54}$$

The final prediction, when written for the dimensionless acceleration $\tilde{a} = a/\langle a^2 \rangle^{1/2}$, becomes [53]

$$p(\tilde{a}) \sim \int_h \tilde{a}^{[h-5+D(h)]/3} R_\lambda^{y(h)} \exp\left(-\frac{1}{2}\tilde{a}^{2(1+h)/3} R_\lambda^{z(h)}\right) \mathrm{d}h, \tag{55}$$

where $y(h) = \chi(h-5+D(h))/6 + 2(2D(h)+2h-7)/3$ and $z(h) = \chi(1+h)/3 + 4(2h-1)/3$. The coefficient χ is the scaling exponent for the Reynolds dependence of the acceleration variance, $\langle a^2 \rangle \sim R_\lambda^\chi$, given by $\chi = \sup_h (2(D(h)-4h-1)/(1+h))$. For the non-intermittent Kolmogorov scaling ($h = 1/3$ and $D(1/3) = 3$), one obtains $\chi = 1$ and (55) recovers the stretched exponential prediction discussed above.

We note that (55) may show an unphysical divergence for $a \to 0$ for many multifractal models of $D(h)$ at small h. This is not a real problem for two reasons. First, the multifractal formalism cannot be extended to very small velocity and acceleration increments because it is based on arguments valid only to within a constant of order 1. Thus, it is not suited for predicting precise functional forms for the core of the PDF. Second, small values of h correspond to very intense velocity fluctuations which have never been accurately tested in experiments or by DNS. The precise functional form of $D(h)$ for those values of h is therefore unknown.

In figure 7 we compare the acceleration PDF computed from the DNS data at $R_\lambda = 280$ with the multifractal prediction (55) using for $D(h)$ an empirical model which fits well the Eulerian scaling exponents [20]. The large number of Lagrangian particles used in the DNS (see [50] for details) allows us to detect events up to $80\sigma_a$. The accuracy of the statistics is
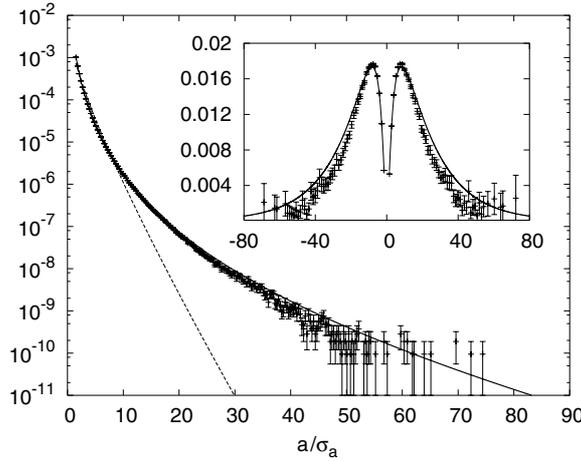
Figure 7. Log-linear plot of the acceleration PDF. Points are the DNS data, the solid line is the multifractal prediction and the dashed line is the K41 prediction. The DNS statistics were calculated along the trajectories of two million particles amounting to 3.6×10^9 events in total. The statistical uncertainty in the PDF was quantified by assuming that fluctuations grow like the square root of the number of events. Inset: $\tilde{a}^4 p(\tilde{a})$ for the DNS data (crosses) and the multifractal prediction.

improved by averaging over the total duration of the simulation and all directions since the flow is stationary and isotropic at small scales. Also shown in figure 7 is the non-intermittent prediction $p(\tilde{a}) \simeq \tilde{a}^{-5/9} R_\lambda^{-1/2} \exp(-\tilde{a}^{8/9}/2)$. As is evident from the figure, the multifractal prediction captures the shape of the acceleration PDF much better than the K41 prediction. What is remarkable is that (55) agrees with the DNS data well into the tails of the distribution—from the order of one standard deviation σ_a up to order $70\sigma_a$. We emphasize that the only free parameter in the multifractal formulation of $p(\tilde{a})$ is the minimum value of the acceleration, $\tilde{a}_{\min}$, here taken to be 1.5. In the inset of figure 7 we make a more stringent test of the multifractal prediction (55) by plotting $\tilde{a}^4 p(\tilde{a})$ and which is seen to agree well with the DNS data.

6. Relative dispersion in turbulence

Relative dispersion of two particles is historically the first issue quantitatively addressed in the study of fully developed turbulence. This was done by Richardson, in a pioneering work on the properties of dispersion in the atmosphere in 1926 [54], and then reconsidered by Batchelor [55], among others, in the light of Kolmogorov 1941 theory [13].

Richardson's description of relative dispersion is based on a diffusion equation for the probability density function $p(\mathbf{r}, t)$, where $\mathbf{r}(t) = \mathbf{x}_2(t) - \mathbf{x}_1(t)$ is the separation of two trajectories generated by (40). In the isotropic case the diffusion equation can be written as

$$\frac{\partial p(\mathbf{r}, t)}{\partial t} = \frac{1}{r^2} \frac{\partial}{\partial r} r^2 K(r) \frac{\partial p(\mathbf{r}, t)}{\partial r}, \tag{56}$$

where the turbulent eddy diffusivity was empirically established by Richardson to follow the 'four-thirds law': $K(r) = k_0 \varepsilon^{1/3} r^{4/3}$ in which k_0 is a dimensionless constant. The scale dependence of diffusivity is at the origin of the accelerated nature of turbulent dispersion: particle relative velocity grows with the separation. The Richardson empirical formula is a

simple consequence of Kolmogorov scaling in turbulence, as first recognized by Obukhov [56].

The solution of (56) for δ-distributed initial condition has the well-known stretched exponential form

$$p(\mathbf{r}, t) = \frac{A}{(k_0 \varepsilon^{1/3} t)^{9/2}} \exp\left(-\frac{9r^{2/3}}{4k_0 \varepsilon^{1/3} t}\right),\tag{57}$$

where $A = 2187/2240\pi^{3/2}$ is a normalizing factor. Of course, the assumption that the relative dispersion can be described by a self-similar process as (56) rules out the possibility of intermittency and therefore the scaling exponents of the moments of relative separation

$$\langle r^{2n}(t)\rangle = C_{2n}\varepsilon^n t^{\alpha_n}\tag{58}$$

have the values $\alpha_n = 3n$, as follows from dimensional analysis. All the dimensionless coefficients C_{2n} are in this case given in terms of k_0 and a single number, such as the so-called Richardson constant C_2, is sufficient to parameterize turbulent dispersion.

The hypothesis of self-similarity is reasonable in the presence of a self-affine Eulerian velocity field, such as in the case of two-dimensional inverse cascade where the dimensional exponents $\alpha_{2n} = 3n/2$ have indeed been found [57]. An analysis of Lagrangian trajectories generated by a kinematic model with synthetic velocity field [58] has shown that Lagrangian self-similarity is broken in the presence of Eulerian intermittency. In this case, it is possible to extend the dimensional prediction for the scaling exponents α_n by means of the multifractal model of turbulence.

From the definition of relative separation

$$\frac{\mathrm{d}}{\mathrm{d}t}\langle r^p(t)\rangle = \langle r^{p-1}\delta v(r)\rangle,\tag{59}$$

where $\delta v(r)$ is the velocity increments between the two trajectories. Using the multifractal representation (7) we can write

$$\frac{\mathrm{d}}{\mathrm{d}t}\langle r^p(t)\rangle \sim \int \mathrm{d}h\, r^{p-1+h+3-D(h)}.\tag{60}$$

The time needed for the pair separation to reach the scale r is dominated by the largest time in the process, associated with the scale r and therefore given by $t \sim r^{1-h}$. This leads to

$$\frac{\mathrm{d}}{\mathrm{d}t}\langle r^p(t)\rangle \sim \int \mathrm{d}h\, t^{[p+2+h-D(h)]/(1-h)}.\tag{61}$$

The integral is evaluated by the saddle point method and gives the final result $\langle r^p(t)\rangle \sim t^{\alpha_p}$ with scaling exponents

$$\alpha_p = \inf_h\left[\frac{p+3-D(h)}{1-h}\right].\tag{62}$$

From the standard inequality of the multifractal formalism (9) one obtains that even in the presence of intermittency $\alpha_2 = 3$. As in the case of single-particle dispersion (50), here also this is a consequence of the presence on the first power of ε in (58) for $n = 1$.

The scaling exponents α_p satisfy the inequality $\alpha_p/p < 3/2$ for $p > 2$. This amounts to say that, as time goes on, the right tail of the particle pair separation probability distribution function becomes narrower and narrower. In other words, due to the Eulerian intermittency particle pairs are more likely to stay close to each other than to experience a large separation.

The multifractal prediction (62) has been checked in the synthetic model of fully developed turbulence [58] where the equivalent Reynolds number is very large. In the case of numerical or experimental data, finite Reynolds effects make very difficult to measure the corrections
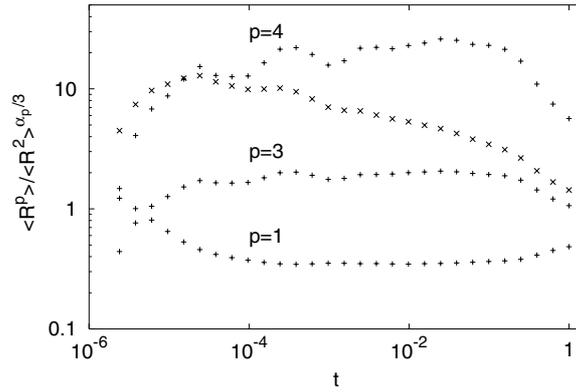
Figure 8. Relative dispersion $\langle r^p(t) \rangle$ rescaled with $\langle r^2(t) \rangle^{\alpha_p/3}$ for $p = 1, 3, 4$ (+) for Lagrangian simulations in a synthetic velocity field corresponding to $R_\lambda \approx 10^6$. The almost constant plateau indicates a relative scaling in agreement with prediction (62). For comparison we also plot $\langle r^4(t) \rangle$ rescaled with the non-intermittent prediction $\langle r^2(t) \rangle^2$ ($\times$) clearly indicating a deviation from normal scaling. Figure from [58].

to dimensional exponents. We remark that finite Reynolds effects are more important in Lagrangian dispersion than in Eulerian statistics: as a consequence of the accelerate nature of relative motion a large fraction of pairs exits the inertial range after a short time.

To overcome these difficulties in Lagrangian statistics, an alternative approach based on exit-time statistics has been proposed for Lagrangian dispersion [58, 59]. In close analogy with the exit-time approach described in section 3.3, one computes the doubling times $T_\rho(R_n)$ for a pair separation to grow from the threshold R_n to the next one $R_{n+1} = \rho R_n$. Averages are then performed over many particle pairs. The outstanding advantage of averaging at fixed scale separation, as opposed to averaging at a fixed time, is that crossover effects are removed since all sampled particle pairs belong to the same scales.

Neglecting intermittency, the doubling time analysis can be used for a precise estimation of the Richardson constant C_2. From the first-passage problem for the Richardson model, (56) one has [60]

$$\langle T_\rho(R) \rangle = \frac{\rho^{2/3} - 1}{2k_0 \varepsilon^{1/3} \rho^{2/3}} R^{2/3} \qquad (63)$$

from which one obtains

$$C_2 = \frac{143}{81} \frac{(\rho^{2/3} - 1)^3}{\rho^2} \frac{R^2}{\varepsilon \langle T_\rho \rangle^3}. \qquad (64)$$

By using this expression it is possible to estimate from DNS data at moderate Reynolds $C_2 = 0.50 \pm 0.05$ [60, 61], which is in agreement with the experimental determination [63].

Intermittency effects are evident in higher order statistics of doubling times. In particular, one expects for the moments of inverse doubling times $\langle (1/T_\rho(R))^p \rangle$ a power-law behavior

$$\left\langle \left(\frac{1}{T_\rho(R)} \right)^p \right\rangle \sim R^{\beta_p} \qquad (65)$$

with exponents β_p connected to the exponents α_n [58]. Negative moments of doubling time are dominated by pairs which separate fast; this corresponds to positive moments of relative separation. By using the simple dimensional estimate $T(R) \sim R/\delta v(R)$ one has the prediction

$$\beta_p = \zeta_p - p, \qquad (66)$$

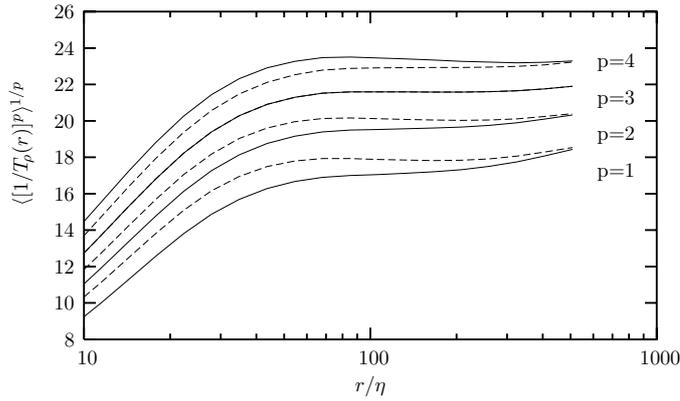where ζ_p are the scaling exponents of the Eulerian structure functions (5).

Figure 9. The inverse exit-time moments, $\langle [1/T_\rho(r)]^p \rangle^{1/p}$, for $p = 1, \ldots, 4$ compensated with the Kolmogorov scalings (solid lines) and the multifractal predictions (dashed lines). Results from DNS at $R_\lambda = 284$, initial particle separation $r_0 = 1.2\eta$ and ratio between exit times $\rho = 1.25$. Figure from [61].

The multifractal prediction (66) is found to be consistent with numerical data at moderate Reynolds number. More important, as shown in figure 9, exit-time statistics is sufficiently accurate for discriminating between intermittent and dimensional scaling in Lagrangian statistics.

7. Dispersion in two-dimensional convection: multifractal analysis of more-than-smooth signals

Thermal convection in two dimensions provides an example of Bolgiano–Obukhov scaling of turbulent fluctuations. Without entering in the details, we recall that within Boussinesq approximation, Bolgiano–Obukhov argument assumes a local balance between buoyancy force and inertial term [64]. In the case of two-dimensional turbulence, in the presence of a mean temperature gradient, Bolgiano–Obukhov scaling is expected to emerge in the inverse cascade of energy with velocity fluctuations given by the scaling law [65]:

$$\delta v(r) \propto \varepsilon_T^{1/5} (\beta g)^{2/5} r^{3/5}, \tag{67}$$

where ε_T is the (constant) flux of temperature fluctuations, β is the thermal expansion coefficient and g is the gravity acceleration. Prediction (67) has been checked in both laboratory experiments [66] and in high-resolution direct numerical simulations [67] which have also shown the absence of intermittency corrections (which is a common feature of two-dimensional inverse cascades).

Now we consider the increments of velocity for Lagrangian tracers transported by Bolgiano turbulence. By extending the dimensional argument of section 4.1 to the general case of velocity scaling exponent h, one obtains [62]

$$\delta v(t) \propto V(t/\tau_0)^{h/(1-h)}. \tag{68}$$

At variance with the Navier–Stokes turbulence, from (67) $h = 3/5$ and therefore $q = h/(1-h) = 3/2 > 1$, i.e. velocity increments in the inertial range are smoother than C_1 signals, the latter denoting the class of differentiable signals. This implies that Lagrangian
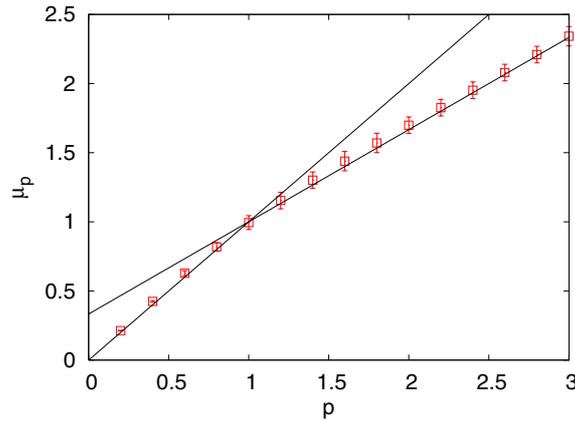
Figure 10. The exit-time scaling exponents μ_p from Lagrangian velocity fluctuations in a DNS of thermal convection with Bolgiano–Obukhov scaling. Lines represent the bifractal prediction (71) and the error bars on the exponents have been estimated by evaluating differences in μ_p changing the fitting interval. Figure from [62].

structure functions (48) are dominated by non-local contributions from the large-scale L which scale as

$$\delta v(t) \sim \tau_L(\partial_t v_L)(t/\tau_L) \tag{69}$$

and therefore give the scaling exponents $\xi_p = p$. This set of scaling exponent is trivially universal for any velocity field with $h > 1/2$ and therefore a standard analysis of Lagrangian velocity fluctuations is unable to disentangle the nontrivial scaling component of the signal [62].

The statistical analysis of more-than-smooth signals has been recently addressed on the basis of an *exit-time statistics* [68] in which one considers the time increments $T(\delta v)$ needed for a tracer to observe a change of δv in its velocity. Now, among the two contributions, in the limit of small $\delta v(t)$, the differentiable part (69) will dominate except when the derivative $\partial_t v_L$ vanishes and the local part (68) becomes the leading one. For a signal with $1 \leqslant q \leqslant 2$, its first derivative is a one-dimensional self-affine signal with Hölder exponent $\xi = q - 1$, which thus vanishes on a fractal set of dimension $D = 1 - \xi = 2 - q$.

Therefore, the probability to observe the component $O(t^q)$ is equal to the probability to pick a point on the fractal set of dimension D, i.e.

$$P(T \sim \delta v^{1/q}) \sim T^{1-D} \sim (\delta v)^{1-1/q}. \tag{70}$$

By using this probability for computing the average p-order moments of exit-time statistics, one obtains the following bifractal prediction [68]:

$$\langle T^p(\delta v)\rangle \sim \delta v^{\mu_p}, \qquad \text{with} \qquad \mu_p = \min\left(p, \frac{p}{q} + 1 - \frac{1}{q}\right). \tag{71}$$

According to prediction (71), low-order moments ($p \leqslant 1$) of the inverse statistics only see the differentiable part of the signal, while high-order moments ($p \geqslant 1$) are dominated by the local fluctuations $O(t^q)$.

Figure 10 shows the first moments of exit times $\langle T^p(\delta v)\rangle$ computed from a direct numerical simulation of two-dimensional Boussinesq equation forced by a mean (unstable) temperature gradient which generates an inverse cascade with Bolgiano–Obukhov scaling.

Particles are advected with (40) and velocity fluctuations are collected along Lagrangian trajectories. The bifractal spectrum predicted by (71) is clearly reproduced. We remark that the fact that for $p > 1$ exponents follow the linear behavior $\mu_p = (2p + 1)/3$ indicates the absence of intermittency in Lagrangian statistics. This feature is a consequence of the self-similarity of the inverse cascade in a two-dimensional Bolgiano convection.

8. Conclusions

Starting from the seminal work of Kolmogorov we considered the statistical features (mainly scaling properties), both Eulerian and Lagrangian, of the fully developed turbulence in the framework of the multifractal model, i.e. in terms of $D(h)$. The hard, still unsolved, problem is, of course, to compute $D(h)$ from first principles. Up to now the unique doable approach is to use multiplicative models motivated by phenomenological arguments. The nontrivial result is the fact that, once $D(h)$ is obtained with a fit of the experimental data from the scaling exponents ζ_p, then the other predictions obtained in the multifractal framework, e.g. the PDF of the velocity gradient, the existence of an intermediate dissipative range, the scaling of Lagrangian structure functions, are well verified.

Acknowledgments

Appendix A. Synthetic turbulence: how to generate multi-affine stochastic processes

In this appendix we describe two methods for the generation of multi-affine stochastic signals [69, 70], whose scaling properties are fully under control. One is based on a dyadic decomposition of the signal in a wavelet basis with a suitable assigned series of stochastic coefficients [69]. The second is based on a multiplication of sequential Langevin processes with a hierarchy of different characteristic times [70].

The first procedure is particularly appealing for modeling of spatial turbulent fluctuations, because of the natural identification between wavelets and eddies in the physical space. The second one looks more appropriate for mimicking the turbulent time evolution in a fixed point of the space.

Using the two methods it is possible to build a rather general $(d + 1)$-dimensional process, $v(\mathbf{x}, t)$, with given scaling properties in time and space.

A.1. An algorithm based and dyadic decomposition

A non-sequential algorithm for a one-dimensional multi-affine signal in $[0, 1]$, $v(x)$, can be introduced as [69]

$$v(x) = \sum_{n=1}^{N} \sum_{k=1}^{2^{(n-1)}} a_{n,k} \varphi\left(\frac{x - x_{n,k}}{\ell_n}\right), \tag{A.1}$$

where we have a set of reference scales $\ell_n = 2^{-n}$ and $\varphi(x)$ is a wavelet-like function [71], i.e. of zero mean and rapidly decaying in both real space and Fourier space. The signal $v(x)$

is built in terms of a superposition of fluctuations, $\varphi((x - x_{n,k})/\ell_n)$ of characteristic width ℓ_n and centered in different points of $[0, 1]$, $x_{n,k} = (2k + 1)/2^{n+1}$. It has been proved [70] that provided the coefficients $a_{n,k}$ are chosen by a random multiplicative process, i.e. the daughter is given in terms of the mother by a random process, $a_{n+1,k'} = X a_{n,k}$ with X a random number identical, independent distributed for any $\{n, k\}$, then the result of the superposition is a multi-affine function with given scaling exponents, namely,

$$\langle |v(x + \ell) - v(x)|^p \rangle \sim \ell^{\zeta_p},$$

with $\zeta_p = -p/2 - \log_2\langle\langle X^p \rangle\rangle$ and $\ell_N \leqslant \ell \leqslant 1$. In this appendix, $\langle\langle \cdot \rangle\rangle$ indicates the average over the probability distribution of the multiplicative process.

Besides the rigorous proof, the rationale for the previous result is simply that due to the hierarchical organization of the fluctuations, one may easily see that the term dominating the expression of a velocity fluctuation at scale R, in (A.1) is given by the couple of indices $\{n, k\}$ such that $n \sim \log_2(R)$ and $x \sim x_{n,k}$, i.e. $v(x + \ell) - v(x) \sim a_{n,k}$. The generalization (A.1) to d dimension is given by

$$v(\mathbf{x}) = \sum_{n=1}^{N} \sum_{k=1}^{2^{d(n-1)}} a_{n,k} \varphi\left(\frac{\mathbf{x} - \mathbf{x}_{n,k}}{\ell_n}\right),$$

where now the coefficients $\{a_{n,k}\}$ are given in terms of a d-dimensional dyadic multiplicative process.

A.2. A sequential algorithm

Sequential algorithms look more suitable for mimicking temporal fluctuations. With the application to time-fluctuations in mind, we will now denote the stochastic one-dimensional functions with $u(t)$. The signal $u(t)$ is obtained by a superposition of functions with different characteristic times, representing eddies of various sizes [70]:

$$u(t) = \sum_{n=1}^{N} u_n(t). \tag{A.2}$$

The functions $u_n(t)$ are defined by the multiplicative process

$$u_n(t) = g_n(t)x_1(t)x_2(t)\cdots x_n(t), \tag{A.3}$$

where $g_n(t)$ are independent stationary random processes, whose correlation times are supposed to be $\tau_n = (\ell_n)^\alpha$, where $\alpha = 1 - h$ (i.e. τ_n are the eddy-turn-over time at the scale ℓ_n) in the quasi-Lagrangian frame of reference [72] and $\alpha = 1$ if one considers $u(t)$ as the time signal in a given point, and $\langle g_n^2 \rangle = (\ell_n)^{2h}$, where h is the Hölder exponent. For a signal mimicking a turbulent flow, ignoring intermittency, we would have $h = 1/3$. Scaling will appear for all time delays larger than the UV cutoff, τ_N, and smaller than the IR cutoff, τ_1. The $x_j(t)$ are independent, positive-defined, identical distributed random processes whose time correlation decays with the characteristic time τ_j. The probability distribution of x_j determines the intermittency of the process.

The origin of (A.3) is fairly clear in the context of fully developed turbulence. Indeed we can identify u_n with the velocity difference at the scale ℓ_n and x_j with $(\varepsilon_j/\varepsilon_{j-1})^{1/3}$, where ε_j is the energy dissipation at the scale ℓ_j [70].

The following arguments show that the process defined according to (A.2) and (A.3) is multi-affine. Because of the fast decrease of the correlation times $\tau_j = (\ell_j)^\alpha$, the characteristic time of $u_n(t)$ is of the order of the shortest one, i.e., $\tau_n = (\ell_n)^\alpha$. Therefore, the leading contribution to the structure function $\tilde{S}_q(\tau) = \langle |u(t + \tau) - u(t)|^q \rangle$ with $\tau \sim \tau_n$ stems from the

nth term in (A.2). This can be understood noting that in $u(t+\tau)-u(t) = \sum_{k=1}^{N}[u_k(t+\tau)-u_k(t)]$ the terms with $k \leqslant n$ are negligible because $u_k(t+\tau) \simeq u_k(t)$ and the terms with $k \geqslant n$ are subleading. Thus, one has

$$\tilde{S}_q(\tau_n) \sim \langle|u_n|^q\rangle \sim \langle\langle|g_n|^q\rangle\rangle\langle\langle x^q\rangle\rangle^n \sim \tau_n^{\frac{hq}{\alpha} - \frac{\log_2\langle\langle x^q\rangle\rangle}{\alpha}}, \tag{A.4}$$

and therefore for the scaling exponents

$$\zeta_q = \frac{hq}{\alpha} - \frac{\log_2\langle\langle x^q\rangle\rangle}{\alpha}. \tag{A.5}$$

The limit of an affine function can be obtained when all the x_j are equal to 1. A proper proof of these results can be found in [70].

Let us note at this stage that the previous 'temporal' signal for $\alpha = 1-h$ is a good candidate for velocity measurements in a Lagrangian, co-moving frame of reference [72]. Indeed, in such a reference frame the temporal decorrelation properties at the scale ℓ_n are given by the eddy-turn-over times $\tau_n = (\ell_n)^{1-h}$. On the other hand, in the laboratory reference frame the sweeping dominates the time evolution in a fixed point of the space and we must use as characteristic times of the processes $x_n(t)$ the sweeping times $\tau_n^{(s)} = \ell_n$, i.e., $\alpha = 1$.

References

[1] Parisi G and Frisch U 1985 *Turbulence and Predictability of Geophysical Fluid Dynamics* ed M Ghil, R Benzi and G Parisi (Amsterdam: North-Holland) p 84
[2] Benzi R, Paladin G, Parisi G and Vulpiani A 1984 *J. Phys. A: Math. Gen.* **17** 3521
[3] Ellis R S 1999 *Physica* D **133** 106
[4] Varadhan S R S *Entropy* ed A Greve, G Keller and D Warnecke (Princeton, NJ: Princeton University Press) p 199
[5] Kolmogorov A N 1962 *J. Fluid Mech.* **13** 82
[6] Novikov E A and Stewart R W 1964 *Izv. Akad. Nauk SSSR Geofiz.* **3** 408
[7] Mandelbrot B B 1974 *J. Fluid Mech.* **62** 331
[8] Beck C and Schögl F 1995 *Thermodynamics of Chaotic Systems* (Cambridge: Cambridge University Press)
[9] Badii R and Politi A 1997 *Complexity: Hierarchical Structures and Scaling in Physics* (Cambridge: Cambridge University Press)
[10] Meakin P 1998 *Fractals, Scaling and Growth far from Equilibrium* (Cambridge: Cambridge University Press)
[11] Harte D 2001 *Multifractals* (Boca Raton, FL: Chapman and Hall)
[12] Halsey T C, Jensen M H, Kadanoff L P, Procaccia I and Shraiman B I 1986 *Phys. Rev.* A **33** 1141
[13] Frisch U 1995 *Turbulence: The Legacy of A. N. Kolmogorov* (Cambridge: Cambridge University Press)
[14] Bohr T, Jensen M H, Paladin G and Vulpiani A 1998 *Dynamical Systems Approach to Turbulence* (Cambridge: Cambridge University Press)
[15] Monin A and Yaglom A 1971 *Statistical Fluid Dynamics* vol I (Cambridge, MA: MIT Press)
     Monin A and Yaglom A 1975 *Statistical Fluid Dynamics* vol II (Cambridge, MA: MIT Press)
[16] Richardson L F 1922 *Weather Prediction by Numerical Processes* (Cambridge: Cambridge University Press)
[17] Kolmogorov A N 1941 *Dokl. Akad. Nauk SSSR* **30** 299
     Kolmogorov A N 1991 *Proc. R. Soc. Lond.* A **434** 9 (reprinted)
[18] Anselmet F, Gagne Y, Hopfinger E J and Antonia R A 1984 *J. Fluid Mech.* **140** 63
[19] Paladin G and Vulpiani A 1987 *Phys. Rep.* **156** 147
[20] She Z S and Lévêque E 1994 *Phys. Rev. Lett.* **72** 336
[21] Aurell E, Frisch U, Lutsho J and Vergassola M 1992 *J. Fluid Mech.* **238** 467
[22] Bender C M and Orszag S A 1999 *Advanced Mathematical Methods for Scientists and Engineers* (New York: Springer)
[23] Frisch U, Martins Afonso M, Mazzino A and Yakhot V 2005 *J. Fluid Mech.* **542** 97
[24] Meneveau C and Sreenivasan K R 1989 *Phys. Lett.* A **137** 103
[25] van de Water W and Schram P 1988 *Phys. Rev.* A **37** 3118
[26] Paladin G and Vulpiani A 1987 *Phys. Rev.* A **35** 1971
[27] Frisch U and Vergassola M 1991 *Europhys. Lett.* **14** 439
[28] Frisch U and She Z-S 1991 *Fluid Dyn. Res.* **8** 139

[29] Castaing B, Gagne Y and Hopfinger E J 1990 *Physica* D **46** 177
[30] Vincent A and Meneguzzi M 1991 *J. Fluid Mech.* **225** 1
[31] Benzi R, Biferale L, Paladin G, Vulpiani A and Vergassola M 1991 *Phys. Rev. Lett.* **67** 2299
[32] Gagne Y and Castaing B 1991 *C. R. Acad. Sci. Ser. II* **312** 441
[33] Biferale L, Cencini M, Vergni D and Vulpiani A 1999 *Phys. Rev.* E **60** R6295
[34] Jensen M H 1999 *Phys. Rev. Lett.* **83** 76
[35] Boffetta G, Cencini M, Falcioni M and Vulpiani A 2002 *Phys. Rep.* **356** 367
[36] Jensen M H, Paladin G and Vulpiani A 1991 *Phys. Rev. Lett.* **67** 208
[37] Shraiman B I and Siggia E D 2000 *Nature* **405** 639
[38] Lamb H 1945 *Hydrodynamics* (New York: Dover)
[39] Tritton D J 1988 *Physical Fluid Dynamics* (Oxford: Oxford Science Publishers)
[40] Maxey M R and Riley J J 1983 *Phys. Fluids* **26** 883
[41] Bec J, Biferale L, Cencini M, Lanotte A S and Toschi F 2006 *Phys. Fluids* **18** 081702
[42] Hénon M 1966 *C. R. Acad. Sci. Paris* A **262** 312
[43] Aref H 1984 *J. Fluid Mech.* **143** 1
[44] Chandrasekhar S 1943 *Rev. Mod. Phys.* **15** 1
[45] Tennekes H and Lumley J L 1972 *A First Course in Turbulence* (Cambridge, MA: MIT Press)
[46] Borgas M S 1993 *Phil. Trans. R. Soc. Lond.* A **342** 379
[47] Boffetta G, De Lillo F and Musacchio S 2002 *Phys. Rev.* E **66** 066307
[48] Mordant N, Metz P, Michel O and Pinton J F 2001 *Phys. Rev. Lett.* **87** 214501
[49] Biferale L, Boffetta G, Celani A, Lanotte A and Toschi F 2006 *J. Turbulence* **7** N6
[50] Biferale L, Boffetta G, Celani A, Lanotte A and Toschi F 2005 *Phys. Fluids* **17** 021701
[51] Benzi R, Ciliberto S, Tripiccione R, Baudet C, Massaioli F and Succi S 1993 *Phys. Rev.* E **48** R29
[52] La Porta A, Voth G A, Crawford A M, Alexander J and Bodenschatz E 2001 *Nature* **409** 1017
[53] Biferale L, Boffetta G, Celani A, Devenish B J, Lanotte A and Toschi F 2004 *Phys. Rev. Lett.* **93** 064502
[54] Richardson L F 1926 *Proc. R. Soc. Lond.* A **110** 709
[55] Batchelor G K 1952 *Proc. Camb. Phil. Soc.* **48** 345
[56] Obukhov A 1941 *Izv. Akad. SSSR Ser. Geogr. Geofiz.* **5** 453
[57] Boffetta G and Sokolov I M 2002 *Phys. Fluids* **14** 3224
[58] Boffetta G, Celani A, Crisanti A and Vulpiani A 1999 *Phys. Rev.* E **60** 6734
[59] Artale V, Boffetta G, Celani A, Cencini M and Vulpiani A 1997 *Phys. Fluids* A **9** 3162
[60] Boffetta G and Sokolov I M 2002 *Phys. Rev. Lett.* **88** 094501
[61] Biferale L, Boffetta G, Celani A, Devenish B J, Lanotte A and Toschi F 2005 *Phys. Fluids* **17** 115101
[62] Bistagnino A, Boffetta G and Mazzino A 2007 *Phys. Fluids* **19** 011703
[63] Ott S and Mann J 2000 *J. Fluid Mech.* **422** 207
[64] Siggia E D 1994 *Annu. Rev. Fluid Mech.* **26** 137
[65] Chertkov M 2003 *Phys. Rev. Lett.* **91** 115001
[66] Zhang J, Wu X L and Xia K Q 2005 *Phys. Rev. Lett.* **94** 174503
[67] Celani A, Mazzino A and Vergassola M 2001 *Phys. Fluids* **13** 2133
[68] Biferale L, Cencini M, Lanotte A, Vergni D and Vulpiani A 2001 *Phys. Rev. Lett.* **87** 124501
[69] Benzi R, Biferale L, Crisanti A, Paladin G, Vergassola M and Vulpiani A 1993 *Physica* D **65** 352
[70] Biferale L, Boffetta G, Celani A, Crisanti A and Vulpiani A 1998 *Phys. Rev.* E **57** R6261
[71] Farge M 1992 *Annu. Rev. Fluid Mech.* **24** 395
[72] L'vov V S, Podivilov E and Procaccia I 1997 *Phys. Rev.* E **55** 7030